Methodology for Numerical Simulation With Cycle-Dependent Relative Permeabilities

J.A. Larsen and **Arne Skauge**, SPE, Norsk Hydro A/S

Summary

Multiphase flow involving saturation oscillations should be modeled with history-dependent, relative permeability functions. Earlier approaches have been based on two-phase flow. The main assumptions have been that the imbibition process is reversible. Moreover, scanning curves were developed only for saturations between some extreme values.

Several tertiary oil recovery processes have shown cycle-dependent hysteresis for relative permeability. When saturation oscillations occur during three-phase flow such as water alternating gas (WAG), the two-phase hysteresis models will generally not be able to describe relative permeabilities obtained from corefloods. For three-phase flow, local hysteresis effects may also be important. New relative permeability representations that account for local hysteresis effects are presented.

Hysteresis models for both wetting and nonwetting phase permeabilities have been developed. The new models account for reduced mobility and irreversible hysteresis loops during three-phase flow. The models depend on the initial saturation at the start of the given process. An algorithm is presented for implementing the nonwetting phase hysteresis model in a numerical simulator. The new three-phase models use experimental wetting and nonwetting relative permeabilities as input, and knowledge of relations between maximum nonwetting saturation and trapped nonwetting saturation.

Introduction

Characteristic parameters describing multiphase flow in porous media are process dependent. In particular, relative permeabilities are considered to be dependent on saturation and saturation history. This latter dependency is described in the literature as relative permeability hysteresis. The number of phases present in porous media is important when discussing hysteresis. The problem of hysteresis increases significantly when moving from two-phase to three-phase flow systems. On a macroscopic scale, the number of process paths increases from two-phase flow to three-phase flow. In addition, the saturation path within the ternary diagram is not predefined in three-phase systems. For the two-phase case, the only unknown part of the saturation trajectory is the endpoint, as compared with three-phase flow, for which the whole saturation trajectory is initially unknown.

On the microscopic scale, displacement sequences that can occur in three-phase systems are not seen in two-phase systems. These include double-displacement mechanisms and the spreading behavior of the intermediate wetting phase. Depending on the equilibrium spreading coefficient, one or two phases can be distributed as films in the porous medium.

Three-phase fluid flow experiments have been analyzed by use of relative permeabilities as functions of one or two phases. Different research groups have reported contradictory trends in data, and several analytical correlation functions exist. The common bases for both interpretation of experiments and analytical correlation functions are relative permeabilities as functions of one- or two-phase saturations and extrapolation of two-phase flow functions to three-phase flow functions. There has been debate on whether the oil relative permeability isoperms are concave or convex, and whether the isoperms are curved or straight lines. Such an interpretation of three-phase flow functions is based on a fluid configuration in which the phases exist in separate cluster structures. The clusters can be replaced intuitively by a network of resistors in which relative permeability is related to the conductivity of the phase clusters. This is known as the channel flow theory,[1] which states that in any flow channel there is at most only one mobile fluid.

New information about fluid flow physics and visual observations from micromodels seem to contradict the channel flow theory.[2-5] Unfortunately, three-phase systems are more complex than is indicated by this theory. Accordingly, the poor agreement between predictions and measurements of three-phase permeabilities can be seen as a symptom of the weakness of the channel flow theory.

This paper is intended to provide new numerical simulation models based on recently presented multiphase flow research.[4-10] The most important theoretical considerations and references are given as examples in the Theoretical Approach section. The experimental results discussed are based mostly on our earlier work. The main results from this section are the qualitative hysteresis trends and the failure of conventional hysteresis models when simulating production and pressure profiles from WAG experiments.

In the Numerical Models section, a detailed description of the new numerical simulation models is presented. The new models are intended for simulation of WAG but should also be valid for other three-phase problems involving water/oil/gas systems. In particular, the gas model can account for changes in gas relative permeability with a water saturation gradient caused by gravity.

Theoretical Approach

Relative permeabilities are generally regarded as saturation dependent, and three-phase relative permeabilities are described as functions of one- or two-phase saturations. Such representations seem to have become an industry standard. Alternative types of functional representations among relative permeability, saturations, and initial saturation point are presented in this section. Hysteresis in relative permeability will then be dependent on the selected functional representation.

The scale over which relative permeabilities are estimated is important. In many cases, the core scale relative permeabilities are only upscaled values based on local volume effects. Saturation directions (that is, increasing or decreasing phase saturations) on the core scale can be significantly different from saturation directions in a local volume element. In the following discussion, relative permeabilities are defined in a local volume element, on a scale appropriate for averaging pore events. It is assumed that a representative elementary volume (REV) always exists. The three-phase hysteresis problem is significantly more advanced than that for two-phase flow, for two reasons: the number of saturation directions increases and the definition of hysteresis becomes ambiguous. The following examples will make these points clearer.

Consistent Description of Relative Permeabilities. Most reservoir simulators use two-phase hysteresis models to predict the imbibition nonwetting-phase relative permeability from the drainage curve. A class of such models has been reported in the literature. Some of the most popular are Carlson's[11] and Killough's[12] models. Another class of models, three-phase relative permeability models or the intermediate-wetting phase (mostly regarded as oil), interpolate two-phase relative permeabilities to estimate three-

Copyright 1998 Society of Petroleum Engineers

Original SPE manuscript received for review 2 April 1997. Revised manuscript received 26 February 1998. Paper (SPE 38456) peer approved 13 March 1998.

phase relative permeabilities. In this class Stone's[1] models are used frequently.

There is a qualitative difference between two-phase hysteresis models and three-phase relative permeability models. For the three-phase case, imbibition and drainage are ambiguous expressions. To classify a three-phase process, increasing or decreasing phase saturation for each phase must be given. The DDI process, for example, consists conventionally of decreasing water saturation, decreasing oil saturation, and increasing gas saturation. To predict oil relative permeability for the DDI process, two-phase oil relative permeability (oil/water and oil/gas) curves have been used. But oil and water saturation cannot both decrease in a two-phase experiment. Like the two-phase hysteresis models, the three-phase models use relative permeabilities for one type of saturation direction to estimate permeabilities for another saturation direction. Can these models be used to understand three-phase hysteresis?

This question cannot be answered yes or no, because the three-phase models are developed from a functional representation that is not well anchored in three-phase flow physics. The next example and **Fig. 1** explain this further.

Consider different DDI processes starting from two different two-phase saturation points, as shown in Fig. 1. These two points can be different steady-state points for the same drainage process. The fluid distribution on the pore level must be different for the two starting points. Assume further that the difference in fluid distributions implies crossing of the two DDI trajectories, as in Fig. 1. Will there be a universal law stating that the relative permeabilities must be equal at the crossing point?

Our answer is probably not. Fluid invasion for small capillary numbers is based on the local capillary pressures, which are dependent on fluid distributions. In other words, it is unlikely that a universal law exists for uniqueness of relative permeabilities at a saturation trajectory crossing point, even if the saturation directions are equal. The following discussion is based on this postulate.

Relative Permeability and Saturation Dependency. Several strategies exist for finding relative permeability saturation functions. During two-phase flow, a saturation trajectory has only one degree of freedom from an initial saturation point, and only one independent saturation exists. Three-phase systems have two independent saturations, and, to be compatible with the two-phase case, relative permeabilities must be defined for every trajectory. The trajectories must be described by saturation directions for each phase, as in a DDI-type expression. That is, no phase can change saturation direction along a trajectory. Such trajectories are named constrained trajectories and are shown in Fig. 1. One major problem with defining relative permeability curves for each constrained trajectory is that the trajectory is not predefined for a given process.

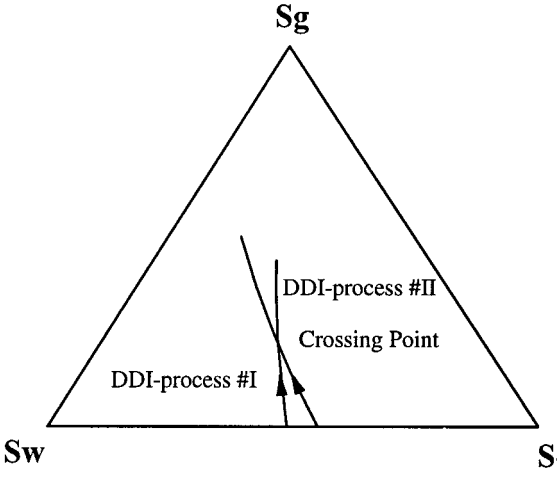

Fig. 1—Two DDI-processes starting from different water and oil saturations. Different initial fluid distributions is assumed to imply that the trajectories are crossing. At the crossing point, relative permeabilities are in general not unique.

From the above discussion it is concluded that three-phase relative permeabilities from different constrained trajectories must be correlated before being used in predictive numerical simulation.

The next problem is to find functional representations for three-phase relative permeabilities from different constrained trajectories. The most used functional representation is

$$k_r = f(S_i, S_j), \quad \ldots\ldots\ldots\ldots\ldots\ldots\ldots\ldots\ldots\ldots\ldots\ldots\ldots\ldots (1)$$

where $i = j$ implies that $k_r = f(S_{i=j})$. The three-phase relative permeabilities are assumed to be functions of one or two saturations. This is the functional basis for Stone's models[1, 13] and the interpretation of experimental studies such as Oak's steady-state experiments.[14]

According to the postulate given earlier, such functional representations are improper for correlating three-phase relative permeabilities. In Fig. 1, two trajectories starting at different initial saturations must have equal relative permeabilities at the crossing point in order for the functional representation in Eq. 1 to be used. It is concluded that functional representation of relative permeabilities (Eq. 1) is not properly anchored in fluid flow physics.

A functional representation according to the postulate is

$$k_r = f(S_i, S^I). \quad \ldots\ldots\ldots\ldots\ldots\ldots\ldots\ldots\ldots\ldots\ldots\ldots\ldots\ldots (2)$$

An even more flexible representation is

$$k_r = f(S_i, S_j, S^I) \quad \ldots\ldots\ldots\ldots\ldots\ldots\ldots\ldots\ldots\ldots\ldots\ldots\ldots\ldots (3)$$

or, if the starting point must be given by two independent saturations,

$$k_r = f(S_i, S_j S^{Ia}, S^{Ib}). \quad \ldots\ldots\ldots\ldots\ldots\ldots\ldots\ldots\ldots\ldots\ldots\ldots\ldots\ldots (4)$$

The difficulty with more flexible functional representations is the increasing number of parameters to be determined. Thus, the later presented hysteresis models use a representation as in Eq. 2. Future experiments for three-phase relative permeabilities should be designed and analyzed with respect to functional representations as in Eqs. 3 and 4. It will then be possible to account for local hysteresis effects.

Fluid Flow at Pore Scale. A question to ask at this point is: What is meant by relative permeability hysteresis? The answer is relatively easy for two-phase systems. Differences in relative permeability are caused by different saturation directions, i.e., drainage and imbibition. This is probably the most reported type of hysteresis. However, it is also possible to have hysteresis between processes with the same saturation direction but separated by one or more saturation-direction changes. An example of the second type of hysteresis is the change in relative permeabilities between primary and secondary drainage.

It is more difficult to define hysteresis in three-phase systems. Differences in relative permeability between constrained trajectories can be a kind of hysteresis, as can differences caused by saturation directions. It would be more practical to investigate the origin of hysteresis effect.

On a microscopic level, in either the wetting or the nonwetting phase, only a fraction of the phase saturation is contributing to the phase conductivity in the porous medium. This fraction has been called flowing fraction or backbone saturation. The rest of the phase saturation is stagnant, occupying dead-end pores or nooks and crannies, and is called the dendritic phase saturation. The nonwetting phase can have an isolated phase fraction in addition to the dendritic fraction of the phase. In gas/oil/water systems, all three phases can be isolated in an intermediate- or mixed-wet porous medium. For water-wet or oil-wet situations, only gas and the nonwetting liquid phase can be isolated. Several authors have pointed out that hysteresis in relative permeability is caused by the difference between processes in backbone saturation (flowing phase fraction). Both experimental approaches[15] and theoretical studies[16] based on network models show that relative permeability plotted against backbone saturation exhibits no hysteresis. Dendritic phase saturation is difficult to measure during an experiment. We do not know of any reported research addressing dendritic

phase saturation for unsteady-state types of displacement experiments. Therefore, the dendritic fluid fraction is not included in any hysteresis models. The following example shows the importance of the dendritic fraction.

This example is based on two-phase hysteresis between drainage and imbibition nonwetting phase relative permeability. Several hysteresis models (Carlson,[11] Killough,[12] etc.) have been developed for this well documented case. Imbibition nonwetting relative permeability is thought to be reduced compared to drainage permeability because of the isolated nonwetting phase saturation. This will be correct only if the nonwetting phase dendritic fraction is equal for drainage and imbibition processes, and at the point where the nonwetting relative permeability is zero (where the dendritic phase saturation also is zero).

The importance of nonwetting phase dendritic saturation can now be illustrated by the difference in drainage-imbibition hysteresis behavior in consolidated and unconsolidated sand, as seen in **Fig. 2**. These two types of porous media are represented by different radius ratios (aspect ratios) between pore bodies and pore throats, where unconsolidated sand typically has a lower aspect ratio than has consolidated sand. If it is only the isolated nonwetting phase that influences phase mobility during imbibition, then both unconsolidated and consolidated sand should show the same quantitative drainage-imbibition hysteresis behavior. However, several authors[17, 18] have reported that imbibition nonwetting phase relative permeability is higher than drainage nonwetting relative permeability for unconsolidated sand and lower for consolidated sand. This is because the ratio of dendritic phase saturation between drainage and imbibition is different in consolidated and unconsolidated sand.

A more complicated case is the three-phase hysteresis between a primary gas injection, G_1, at irreducible water saturation and oil saturation, a subsequent water injection, W_2, and a tertiary gas, G_3. Skauge and Larsen[10] have reported relative permeabilities for these processes. Another possible injection sequence related to WAG is a primary water injection, W_1, followed by a secondary gas injection, G_2. G_1, G_2, and G_3 will all be DDI processes (at least on the core scale), but, generally, the gas relative permeability is different.

A detailed interpretation of hysteresis based on pore-level effects is not within the scope of this paper. Such analysis is very complicated, and more research is needed. The last example gives some important characteristics of the pore level in relative permeabilities.

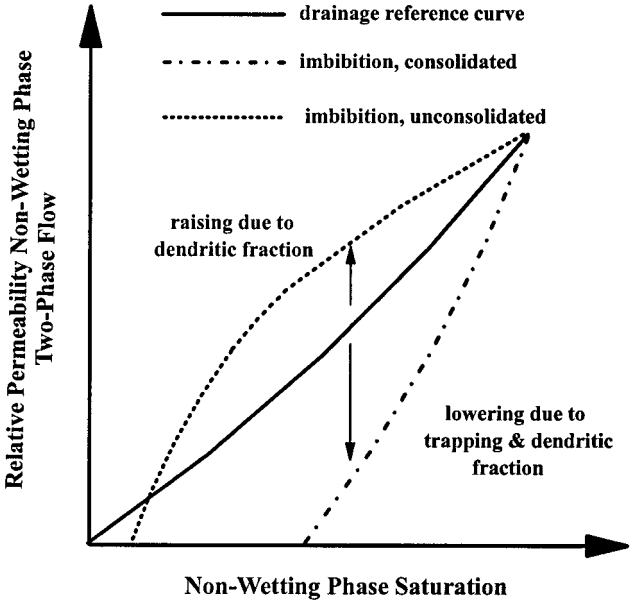

Fig. 2—Different two-phase hysteresis behavior between consolidated and unconsolidated sand. Drainage curve is only for reference and is generally not equal for the two types of porous media.

The difference between gas relative permeability from G_1 and G_2 processes is studied. Primary gas injection, G_1, is performed with no initial trapped nonwetting saturation. G_2 starts with oil previously trapped in the large pores by a W_1 process. These two cases give different local capillary pressures.[8] For the G_1 case, oil exists in a continuous cluster from inlet to outlet. Because gas is assumed to be the nonwetting phase, the larger oil-filled pores will be invaded first. Depending on pore size distributions and pore-to-pore correlations, the G_2 process, in contrast, will tend to displace water from smaller water-filled pores. Invasion of larger pores with trapped oil involves a double displacement with gas/oil/water. A double displacement is constrained by the sum of gas/oil capillary pressure and oil/water capillary pressure.[4]

Gas permeability from the G_2 process is, accordingly, observed to be lower than that from the G_1 process.[10] Furthermore, experimental studies[5, 20] have concluded that gas permeability is lower for a nonspreading system than for a spreading system. The spreading conditions are important for the formation of stable oil layers between water and gas. However, new results[7, 19] show that the formation of oil layers is dependent on the capillary pressures. As shown in **Fig. 3**, the capillary pressure regimes for G_1 and G_2 are different. The arguments follow from an idealized pore model without viscous forces, which is implemented in a rule-based network simulator.[7] It is then possible to have DDI processes starting at different water/oil saturations that do not have the same oil layer behavior.

With the pore-level model, experimental results regarding gas hysteresis, based on different spreading conditions,[5, 20] are in qualitative agreement with hysteresis caused by different process paths.[10]

Experimental Observations

This section summarizes experimental results from two- and three-phase hysteresis.

Relative Permeability for Nonwetting Phase. The nonwetting phase refers to either oil or gas in two-phase flow, but it refers specifically to the gas phase for three-phase systems.

Many researchers have reported hysteresis behavior of nonwetting phase (oil) relative permeability in two-phase systems. The dependence of nonwetting phase permeability on the saturation history was pointed out by Geffen *et al.*[21] and Osoba *et al.*[22] These authors noted that saturation history affects the statistical saturation distribution of the fluids in the pore space.

Kyte *et al.*[23] reported trapped gas measurements in two- and three-phase systems, and found that, for a given porous medium and fluid system, there is a unique relationship between the trapped gas saturation and the initial free gas saturation. The trapping process was found to be independent of oilflooding or waterflooding. On the basis of published data from Kyte *et al.*,[23] Holmgren and Morse,[24] Dyes,[25] Dardaganian,[26] and Crowell *et al.*,[27] Land[28]

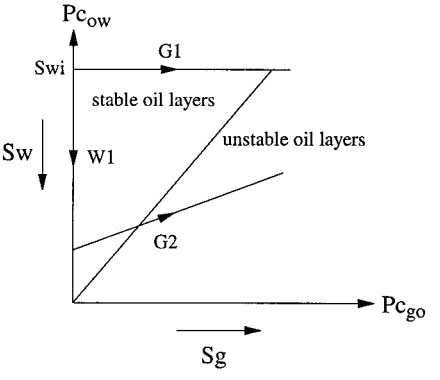

Fig. 3—Relative permeability to gas is dependent on process path through capillary pressure regimes, the line between stable and unstable oil layers is dependent on contact angles, interfacial tension, equilibrium spreading coefficient, and geometrical features of the pore.

formulated the following empirical relation between initial gas saturation, S_{gi}, and trapped gas saturation, S_{gr}.

$$\frac{1}{S_{gr}} - \frac{1}{S_{gi}} = C \quad \ldots\ldots\ldots\ldots\ldots\ldots\ldots\ldots\ldots\ldots\ldots\ldots\ldots\ldots (5)$$

where C = a constant.

Land[28] separated the gas saturation into two parts: free gas saturation contributing to flow and trapped gas saturation. He showed that the free gas saturation can be expressed as a function of S_g with S_{gr} and C as parameters (see, e.g., Carlson[11]):

$$S_{gf} = \frac{1}{2}\left[(S_g - S_{gr}) + \sqrt{(S_g - S_{gr})^2 + \frac{4}{C}(S_g - S_{gr})} \right]. \quad \ldots\ldots (6)$$

Eq. 6 is valid in a decreasing immiscible nonwetting saturation process and is generally not restricted to gas being the nonwetting phase. Land[28] used S_{gf} to express the imbibition (decreasing gas saturation) gas relative permeability, but he did not connect the drainage (increasing gas saturation) and imbibition processes in a hysteresis model. The free gas saturation can be seen as an analog to flowing fraction.

Naar *et al.*[17] observed a difference in relative permeability when drainage and imbibition processes were repeated. The imbibition curve was retraced only when these processes were applied to an unconsolidated sand. Evrenos and Comer[29] studied numerical simulations of hysteresis and also addressed the impact of multicyclic saturations on two-phase relative permeability. They found no significant difference of nonwetting relative permeability when drainage and imbibition processes were repeated independent of consolidated or unconsolidated sand. Colonna *et al.*[30] observed an additional hysteresis phenomenon, along with the standard imbibition-drainage hysteresis reported in capillary pressure, when a first drainage was followed by a total (down to residual nonwetting phase) imbibition and a new secondary drainage was performed. They did not report similar observations for relative permeabilities. Killough[12] connected, for the first time, the Land relation (Eq. 6) with the concept of a dynamic hysteresis envelope consisting of bounding drainage and bounding imbibition curves and intermediate scanning curves. Killough[12] assumed that the imbibition curve is retraced when nonwetting phase saturation is increasing after a decreasing process, although he could not find unique experimental data to support this. Finally, Carlson[11] extended the Land theory, such that the bounding imbibition curve and scanning imbibition curves are calculated from the given drainage curve and the Land constant. This can be done by setting

$$k_{rg}^{\text{imb}}(S_g) = k_{rg}^{\text{drain}}(S_{gf}), \quad \ldots\ldots\ldots\ldots\ldots\ldots\ldots\ldots\ldots\ldots (7)$$

where S_{gf} = estimated from Eq. 6. It is then assumed that the dendritic phase saturation is equal for both imbibition and drainage. In this case, all imbibition scanning curves become parallel.

The majority of publications about relative permeability hysteresis are restricted to two-phase imbibition-drainage hysteresis. Little effort has been made to investigate cycle-dependent hysteresis. In three-phase flow, the investigations are mostly limited to determination of relative permeability isoperms and their dependence on one or two phases. Very few researchers have reported hysteresis phenomena in multicyclic three-phase systems.

Eikje *et al.*[31] studied relative permeability in three-phase water/oil/microemulsion displacement experiments. The relative permeabilities were interpreted by Virnovskii's[32] theory. They concluded from their experimental data that it is necessary to include irreversible hysteresis loops for both wetting (water) and nonwetting (oil) phases. They found a significant drop in nonwetting phase permeability between hysteresis loops when two phases were mobile as compared with hysteresis loops obtained for three-phase flow. Experimental data from Kvanvik *et al.*[33] may support this observation, but exact conclusions cannot be drawn because of the varying capillary number. Generally, much less hysteresis is observed for the nonwetting phase than was seen in the work reported by Eikje *et al.*[31]

Both field and laboratory results have shown cycle-dependent relative permeabilities. Low fluid mobilities from field observations and injectivity decline during CO_2 tertiary floods have been reported by several authors.[34, 35] Hawkins and Bouchard[36] reported laboratory studies with cycle-dependent two-phase hysteresis from unsteady-state measurements on a synthetic core. They controlled conditions so that no wettability alterations occurred during the experiment. Their observations were the same as those in the work of Patel *et al.*[34]: a significant decrease in mobility between the first and second displacement cycles. The synthetic core was assumed to be oil-wet. Braun and Holland[37] investigated relative permeability hysteresis on water-wet and mixed-wet cores by means of a steady-state technique. They found that the imbibition nonwetting permeability was retraced by a subsequent drainage only for the water-wet condition.

Several experimental studies[9, 10] of three-phase flow have concluded that gas relative permeability may be strongly reduced (by, at most, a factor of 10) from two-phase gas drainage (at S_{wi}; G_1) to drainage after waterflooding (G_3). The trapping of oil seems to restrict the flow of gas. However, wettability is assumed to be an important factor in gas relative permeability in three-phase flow, because it determines the local distribution of the oil phase. A three-phase gas relative permeability model should therefore incorporate dependency of water saturation to be able to describe cases in which water reduces gas permeability during hysteresis cycles.

Concept of Hysteresis Treatment for Nonwetting Phase. We have found evidence of cycle-dependent hysteresis from both our own studies and others, involving many different types of fluids, rock properties, and experimental conditions. The results range from coreflood to field behavior. Generally, porous media deviating from an extreme water-wet condition show stronger cycle-dependent relative permeability.

The results from unsteady-state experiments and the above discussion suggest that predictive three-phase gas permeability models are dependent not only on increasing or decreasing gas saturation, but also on water saturation history. This leads to the following assumption in numerical simulation: the dependence of water saturation on gas mobility is restricted to the water saturation at the start of a hysteresis loop. A hysteresis loop starts with DDI, with a following total IDD. Increasing water saturation during gas saturation cycles will reduce the mobility to gas in three-phase systems compared with two-phase systems.

Relative Permeability for Wetting Phase. Generally, the wetting phase refers to water and is thought to have less drainage-imbibition hysteresis than the nonwetting phase[32] because it cannot be trapped or disconnected in natural porous media.

Studies of two-phase flow[37, 38] have shown increased water-phase hysteresis at intermediate wettability. Different capillary numbers have been reported to influence water relative permeability hysteresis.[39, 40] Larger hysteresis was observed in the water phase with low capillary numbers. In all cases, less drainage-imbibition hysteresis in the nonwetting phase was observed for increasing capillary numbers.[39-41]

There can be some confusion about hysteresis related to initial saturation of the core. Most of the two-phase studies refer to the primary process as starting with a core completely saturated with wetting phase, and the flooding sequence becomes a first or primary drainage down to irreducible wetting-phase saturation followed by an imbibition. From this point, a second cycle can be activated. In our work[10] regarding three-phase hysteresis, the initial saturation of the core is two-phase oil and water at irreducible saturation. It is not likely that the cycle-dependent hysteresis in two-phase systems discussed above can be related directly to three-phase flow because stable/unstable layers of intermediate phase do not exist in two-phase systems.

Wang[42] reported trapping of water in a mixed-wet porous medium by means of a convection-diffusion equation to fit tracer-effluent profiles. Trapping of water, thereby reducing water mobility, can occur in a non-water-wet reservoir if, for example,

residual oil saturation decreases in the presence of three-phase alternating flow when an oil bank is mobilized.

In the case of miscible displacement in both sandstone and carbonates, attention in the literature has been focused on reduced post-solvent waterflood injectivities compared with those observed during water preinjection. Schneider and Owens[35] reported a five-fold reduction of water mobility in a three-phase flow situation compared with a two-phase flow in moderately oil-wet carbonates from four West Texas reservoirs. This reduction resembles field evidence of reduced water injectivity. Although in many field cases, reduced water injectivity has not been observed, field observations may be dominated by other effects such as thermal fractures.

Killough[12] developed a hysteresis scheme for the wetting phase in two-phase systems. The imbibition process is assumed to be reversible, and hysteresis occurs only when a first drainage process is reversed to imbibition. This makes the Killough wetting-phase model less useful in three-phase flow problems because, if the first process occurring in the porous medium is imbibition from an initial irreducible wetting-phase saturation, hysteresis cannot be included at a later point. Clearly, no cycle-dependent hysteresis can be included in the Killough model.

When the same notation as that in the previous section is used, relative permeability to water from W_1 is significantly larger than water permeability from W_2 and W_3 processes in an intermediate/mixed wet sandstone.[10] These observations can be based on different dendritic structures of the water phase, but the possibility of water trapping in these mixed-wet systems should be investigated further. A three-phase water relative permeability model should therefore incorporate dependence of gas saturation to be able to describe cases in which gas reduces water permeability.

Hysteresis Treatment for the Wetting Phase. The water relative permeability effects are based on process dependence, which cannot be properly included if the water permeability is allowed to be a function of more than one phase saturation. There are not enough experimental data relating water relative permeability for many different processes to the initial condition of each process. Because of a lack of functional dependencies, saturation-interpolated scanning curves are used between known water relative permeability curves.

In the proposed hysteresis model, the reduction of water permeability is connected to the gas saturation, in accordance with experimental observations. Water permeability for the increasing water saturation process depends on gas saturation at the start of the process, and water permeability for the decreasing water saturation process depends on gas saturation as a free variable. The proposed model reduces to a two-phase behavior if the gas saturation value is zero.

Relative Permeability for Intermediate Wetting Phase. Mathematical models that can estimate three-phase oil relative permeability from two-phase permeabilities have been used extensively in numerical simulations.[1, 13] Many investigators have pointed out that these models fail to predict experimental measured three-phase oil relative permeabilities,[43, 44] and in many cases, linear interpolation between two-phase data is an equally effective approach.

In WAG coreflood studies, extreme low endpoint oil saturation is observed.[9] In fact, the oil remaining after only 2 pore volume (PV) of WAG injection can be below 5% PV, whereas the remaining oil after an equivalent number of PV with continuous gas, G_1, or water, W_1, injection is about 20 to 40% in primary processes. Consequently, there is a saturation domain from an oil saturation of about 5 to about 30%, in which two-phase data cannot give any information at all about three-phase flow. Setting the residual oil saturation to 30% in numerical simulations of those WAG corefloods is clearly inaccurate, but setting residual oil saturation to about zero also has a disadvantage because some parts of a reservoir can behave like a primary process. In the case of secondary and tertiary gas (G_2-G_3) and water (W_2-W_3) injections, which are also three-phase processes, the remaining oil is typically 10 to 40%.

As noted above in the section entitled Theoretical Approach, a difference is expected in stable oil layers independent of displacement series G_1-W_2 and W_1-G_2. We explained reduction of gas relative permeabilities by early trapping of oil from unstable oil layers. Another indication that this theory contains important mechanisms for fluid behavior is shown by comparing residual oil after the G_1-W_2 and W_1-G_2 displacement series. As expected, the water displacement after gas gives significantly lower residual oil than does gas displacement after water (see **Table 1**).

Reservoir simulation of the WAG process[45, 46] shows that some areas will be gasflooded or waterflooded or will exhibit WAG depending on vertical and horizontal positions. Then, the residual oil saturation will differ in these regions depending on whether WAG, water, or gas flow is the major process. Can this problem be managed by separating the reservoir into regions and using analytical approaches[47, 48] to address special relative permeabilities in these regions?

First, the analytical models cannot account for the difference in phase mobility of gas and water caused by hysteresis effects. Second, the saturation distribution in the regions is assumed to be uniform, and oil relative permeability is not considered. Then, the different regions can only be known through a correct WAG simulation model. We conclude that an oil relative permeability model accounting for WAG effects and two-phase flow, together with appropriate hysteresis models for gas and water, is the best way to characterize the performance of WAG in field studies. Guzman *et al.*[49] have shown by numerical simulation that the three-phase region during WAG injection depends on the three-phase relative permeability model.

Neither of Stone's methods, 1[1] or 2,[13] can reproduce the low residual oil saturation. The first model offers the flexibility of having an input, given residual oil saturation, but in the second Stone model, the residual oil saturation is given from the equation itself. This gives the first model a significant advantage in numerical simulation. Holmgren and Morse[24] were the first to report that residual oil by waterflood is higher than residual oil after a waterflood with initial free gas. Linear interpolation[50] between two-phase gas/oil and water/oil residual saturation has been proposed in Stone's Method 1. In three-phase water/oil/gas systems, an empirical relationship between residual oil saturation, residual oil by waterflood, and trapped gas seems to exist.[50]

$$S_{or} = S_{orw} - aS_{gt}, \quad \ldots\ldots\ldots\ldots\ldots\ldots\ldots\ldots\ldots\ldots (8)$$

where a = a constant.

The value of the constant has been suggested to be both 0.5[50] and equal to unity[9, 51] in water-wet systems. Our data (Table 1) suggest

TABLE 1—IMPACT OF TRAPPED GAS SATURATION ON RESIDUAL OIL

Core Material	Wettability	a (from Eq. 26) WAG	a (from Eq. 26) Continuous Injection	Residual Oil G_1-W_2	Residual Oil W_1-G_2
Berea	Water-wet	0.5	0.4	0.08	0.44
Reservoir 1	Water-wet	0.5	0.3	0.20	0.36
Reservoir 2	Water-wet	1.1	0.4	0.30	0.23
Reservoir 3	Mixed-wet	1.1	0.9	0.16	0.18

a value of 0.3 to 0.5 in water-wet sandstone and about unity for intermediate wetting sandstone in the case of continuous injections W_1-G_2-W_3, where the residual oil is taken after tertiary water injection. In the case of WAG, the effect of trapped gas seems to reduce residual oil more effectively than continuous injection. This cannot be properly explained by the capillary pressure regime and process path theory discussed in earlier sections. However, this simplified theory neglects viscous forces and their influence on relative permeability behavior. To understand the WAG process, this issue must be included in further research, and better three-phase oil relative permeability models for numerical simulation can be made.

Numerical simulation with Eq. 8 to determine residual oil will be invalid if the process studied is different from the process in which the constant is estimated. As pointed out earlier, on a reservoir scale, different processes will be valid in certain regions.

Numerical Models

Numerical Model for Nonwetting Phase. The numerical model attempts to reproduce qualitatively the hysteresis behavior in the gas phase. To have an effective code, some limitations and simplifications must be submitted in the numerical model. Although this new model uses different scanning curves for increasing and decreasing gas saturation, a scanning curve for decreasing gas saturation is calculated from the scanning curve for increasing gas saturation in the same hysteresis loop. The primary gas relative permeability curve, G_1, is used together with Land's relation (Eq. 5) to generate both types of scanning curves. Accordingly, both the G_1 curve and the Land constant, C, must be given as inputs to the numerical model.

The main feature of the new model is reduction of gas mobility during hysteresis loops in the presence of increasing water saturation. Then, the gas relative permeability can be reduced because of trapping. The Land formalism is maintained and is essential in the trapped gas estimation procedure.

Scanning Curves for Increasing Gas Saturation (Drainage). All increasing gas saturation scanning curves can be calculated from

$$[k_{rg}^{\text{drain}}(S_g, S_w^{\text{I}}; S_g^{\text{start}})]_n = \left\{[k_{rg}^{\text{input}}(S_g) - k_{rg}^{\text{input}}(S_g^{\text{start}})]*\left(\frac{S_{wi}}{S_w^{\text{I}}}\right)^{\alpha}\right\}_n + [k_{rg}^{\text{imb}}(S_g^{\text{start}})]_{n-1}, \quad \ldots\ldots\ldots\ldots\ldots\ldots (9)$$

where $S_g \in [S_g^{\text{start}}, 1]$. The primary gas relative permeability curve, G_1, exists from $S_g = 0$ to a maximum value of gas saturation. Then, the first pair of parentheses on the right side of Eq. 9 represents a transformation of the G_1 curve at $S_g = S_g^{\text{start}}$, such that the G_1 curve becomes zero at $S_g = S_g^{\text{start}}$. The second set of parentheses is a reduction part, which accounts for the reduction of gas relative permeability in the presence of mobile water. This implies that gas relative permeability is coupled to both the historical water saturation and gas saturations, but is not a function of the present water saturation.

The last term in Eq. 9 is the stopping point of the last hysteresis loop. This term ensures continuity between the hysteresis loop $n-1$ and n. When $n = 1$, this term is zero if the first process observed in the system is an increasing gas saturation process. If the first process observed in the system is a decreasing gas saturation process, the expression $[k_{rg}^{\text{imb}}]_{n=0}$ (note that the first hysteresis loop, $n = 1$, is defined to start with increasing gas saturation) will exist, and must be accounted for in Eq. 9. The concept of hysteresis loops is shown in **Fig. 4**. The end of a hysteresis loop is always defined as the point where the corresponding scanning curve for decreasing gas saturation intersects the S_g-S_w plane (total imbibition $k_{rg} = 0$). Note that the decreasing gas saturation process can stop before reaching the endpoint of the hysteresis loop. In such a case, the starting point of loop n, $(S_g^{\text{start}})_n$, will not be equal to the endpoint of loop $n-1$, $(S_g^{\text{end}})_{n-1}$.

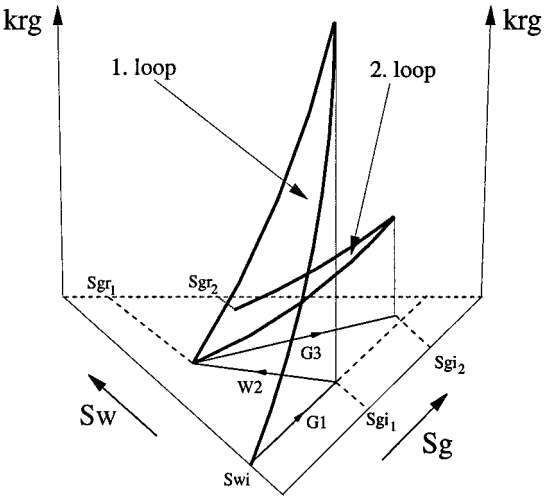

Fig. 4—Hysteresis loops during three-phase flow with reduction of gas permeability.

Scanning Curves for Decreasing Gas Saturations (Imbibition). Now that we have established a theory for developing drainage scanning curves, the procedure for calculating imbibition curves (or, more precisely, scanning curves for decreasing gas saturation) must obey the trapped gas formalism of Land. This involves transformation of gas saturations in the following manner.

$$(S_g^{\text{trans}})_n = (S_g)_n - (S_g^{\text{end}})_{n-1}, \quad \ldots\ldots\ldots\ldots\ldots\ldots (10a)$$

where $(S_g)_n \in [(S_g^{\text{end}})_{n-1}, (S_{gi})_n]$; $\ldots\ldots\ldots\ldots\ldots\ldots (10b)$

$$(S_{gr}^{\text{trans}})_n = (S_{gr})_n - (S_g^{\text{end}})_{n-1}; \quad \ldots\ldots\ldots\ldots\ldots\ldots (11)$$

$$(S_{gi}^{\text{trans}})_n = (S_{gi})_n - (S_g^{\text{end}})_{n-1}; \quad \ldots\ldots\ldots\ldots\ldots\ldots (12)$$

and $$(C^{\text{trans}})_n = \frac{1}{(S_{gr}^{\text{trans}})_n} - \frac{1}{(S_{gi}^{\text{trans}})_n}. \quad \ldots\ldots\ldots\ldots\ldots\ldots (13)$$

Eq. 7 can be used with transformed saturations [note that the $(S_g^{\text{end}})_{n-1}$ cancels out in the saturation parts].

$$\left\{S_{gf} = \frac{1}{2}\left[(S_g - S_{gr}) + \sqrt{(S_g - S_{gr})^2 + \frac{4}{C^{\text{trans}}}(S_g - S_{gr})}\right]\right\}_n. \quad \ldots\ldots\ldots\ldots\ldots\ldots (14)$$

Then, the transformed free saturation can be calculated as

$$(S_{gf}^{\text{trans}})_n = (S_{gf})_n + (S_g^{\text{end}})_{n-1}. \quad \ldots\ldots\ldots\ldots\ldots\ldots (15)$$

The relative permeability can now be calculated from a similar expression, as in Eq. 4, with S_{gf} replaced by S_{gf}^{trans}.

$$[k_{rg}^{\text{imb}}(S_g) = k_{rg}^{\text{drain}}(S_{gf}^{\text{trans}})]_n, \quad \ldots\ldots\ldots\ldots\ldots\ldots (16a)$$

where $S_{gf}^{\text{trans}} \in [(S_g^{\text{start}})_n, (S_{gi})_n]$. $\ldots\ldots\ldots\ldots\ldots\ldots (16b)$

With this procedure the Land formalism is still valid, i.e., trapped gas is estimated directly from Eq. 4.

One problem arises when $S_{gf}^{\text{trans}} < S_g^{\text{start}}$ is a decreasing gas saturation process, because k_{rg}^{drain} does not exist for these saturations. In this domain, the imbibition scanning curve from the former hysteresis loop ($n-1$) must be adopted as an associated drainage scanning curve. Clearly, this is a point at which assumptions are made to simplify the numerical model.

$$[k_{rg}^{\text{imb}}(S_g)]_n = [k_{rg}^{\text{imb}}(S_{gf}^{\text{trans}})]_{n-1}, \quad \ldots\ldots\ldots\ldots\ldots\ldots (17a)$$

where $S_{gf}^{\text{trans}} \in [(S_{gr})_n, (S_g^{\text{start}})_n]$. $\ldots\ldots\ldots\ldots\ldots\ldots (17b)$

Small saturation oscillations, which normally should not influence the gas relative permeability, can give erroneous effects in a

hysteresis model. New hysteresis loops, starting from conditions other than the original loop, can be generated from these small oscillations. An example of the small oscillation problem is given in **Fig. 5**. The small saturation oscillations can be divided in two parts, depending on origin: oscillations caused by numerical instabilities and system-dependent oscillations. Gas saturation oscillations caused by numerical instabilities will be avoided by using tolerance limits for generating hysteresis loops. Oscillations in gas saturation originating from the physical system must, however, be properly handled. In this case, taking the limit (gas saturation oscillation) $\rightarrow$ (tolerance limit), no large changes in gas mobility should occur. In a three-phase situation, decreasing gas saturation can result from increasing/increasing/decreasing (IID), increasing/decreasing/decreasing (IDD), or decreasing/increasing/decreasing (DID) processes. Unfortunately, there is no experimental evidence explaining the influence of these processes on gas mobility during small saturation oscillations. However, the DID process (e.g., a process involving an oil bank) will probably decrease the effect of reduced gas mobility because of decreasing water saturation. The two other processes are probably more connected to the maximum historical water saturation in the system (i.e., the original blocked gas channels). Therefore, the final gas mobility should not be changed when IID and IDD processes occur if no new historical maximum of water saturation is reached. If 1 and 2 represent, respectively, the start and endpoint of an imbibition process as in Fig. 5, the following criterion exists: if $(S_g^1 - S_g^2) \geqq (S_o^2 - S_o^1) + \varepsilon$ and $S_w^2 < S_w^{\max}$, then the imbibition curve is retraced to the inflection point, and the (former) drainage curve is followed, or else a new hysteresis loop is generated. In Fig. 5, the path 1-2-1-3′ is followed if the above criterion is fulfilled; otherwise, the path 1-2-3 is followed.

Constraints. If the studied process starts with increasing gas saturation, Eq. 9 is used to calculate the corresponding drainage curve. In this case, the last term on the right side of Eq. 9 becomes zero.

If the studied process starts with decreasing gas saturation, the corresponding imbibition scanning curve from the primary drainage curve is calculated by Eqs. 7 and 8. The Land constant must be given as input.

If an increasing gas saturation process does not reach the historical maximum gas saturation, the drainage scanning curve is retraced by the following decreasing gas saturation process and no imbibition scanning curve is calculated.

Numerical Model for the Wetting Phase. Inputs to the numerical model are a primary water relative permeability curve, W_1, and a secondary water relative permeability curve, W_2, after gas injection. The initial saturation state for the primary process is irreducible water and oil and the W_1 process is, accordingly, a two-phase flow case. Gas saturation at the start of the three-phase W_2 process (IDD) must be known, and it is denoted as maximum gas saturation $(S_g)^{\max}$. The Land constant must also be known such that $(S_{gr})^{\max}$ can be calculated. The input curves are given in **Fig. 6**. From these curves all other water relative permeability curves for increasing water saturation can be calculated depending on initial gas saturation.

Scanning Curves for Increasing Water Saturation (Imbibition). The scanning curves for increasing water saturation, as shown in Fig. 7, are interpolated from $k_{rw^1}^{W}$ and $k_{rw^2}^{W}$.

$$[k_{rw}^{\text{imb}}(S_w; S_g^{\text{I}})] = k_{rw}^{W_1}\left[1 - \frac{S_g^{\text{I}}}{(S_g)_{\max}}\right] + k_{rw}^{W_2}\left[\frac{S_g^{\text{I}}}{(S_g)_{\max}}\right]. \quad \ldots\ldots\ldots (18)$$

Here, S_g^{I} = the gas saturation at the start of the increasing water saturation process. If the porous medium is in a two-phase oil/water situation, the W_1 curve will be followed. At the end of the first increasing water saturation process with an initial gas saturation larger than zero and smaller than the maximum gas saturation, the water relative permeability will be at Point A in **Fig. 7**. For an initial gas saturation equal to zero or the maximum gas saturation, the bounding curves W_1 and W_2, respectively, will be used.

Scanning Curves for Decreasing Water Saturation (Drainage). There are three displacement cycles for decreasing water saturation that must be considered; increasing gas saturation, decreasing gas saturation (oilflood), and constant gas saturation. The gas saturation at the start of the drainage process, S_g^{I}, determines the water permeability hysteresis behavior. Note that, here, the initial gas saturation generally is different from the increasing water saturation process, although the same notation is used.

1. $(S_g - S_g^{\text{I}}) > 0$ gasflood, curve AB in Fig. 7,

$$(k_{rw}^{\text{drain}}) = (k_{rw}^{\text{imb}})_f\left(1 - \frac{S_g - S_g^{\text{I}}}{(S_g)_{\max} - S_g^{\text{I}}}\right) + k_{rw}^{W_2}\left(\frac{S_g - S_g^{\text{I}}}{(S_g)_{\max} - S_g^{\text{I}}}\right). \quad \ldots\ldots\ldots (19)$$

2. $(S_g - S_g^{\text{start}}) < 0$ oilflood, curve AD in Fig. 7,

$$(k_{rw}^{\text{drain}}) = (k_{rw}^{\text{imb}})_f\left(1 - \frac{S_g^{\text{I}} - S_g}{S_g^{\text{I}}}\right) + k_{rw}^{W_1}\left(\frac{S_g^{\text{I}} - S_g}{S_g^{\text{I}}}\right). \quad \ldots\ldots\ldots (20)$$

3. Constant gas saturation, curve AC in Fig. 7,

$$(k_{rw}^{\text{drain}}) = (k_{rw}^{\text{imb}})_f. \quad \ldots\ldots\ldots (21)$$

Note that $(k_{rw}^{\text{imb}})_f$ is the relative permeability curve from the last (former) increasing water saturation process. At Condition 3 above, no hysteresis occurs between increasing and decreasing water saturation processes. Although this assumption is made for numer-

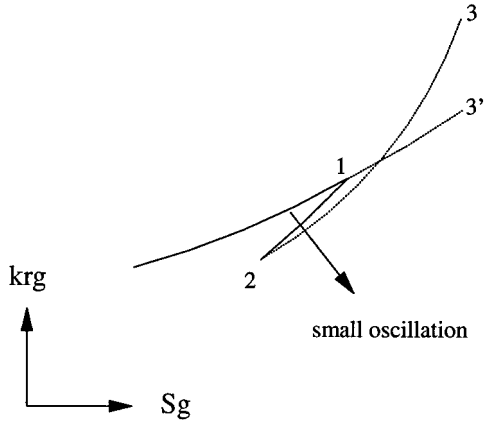

Fig. 5—Hysteresis loops generated by small oscillations in gas saturation.

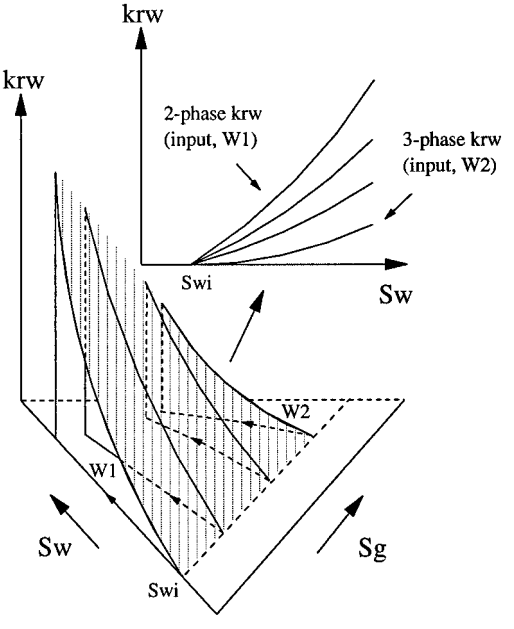

Fig. 6—Input functions and relative permeability surface for increasing water saturation.

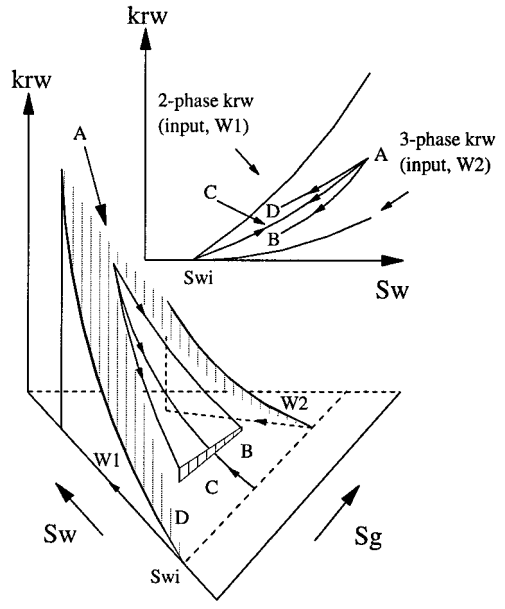

Fig. 7—Hysteresis loops for decreasing water saturation.

ical convenience, it can also be supported empirically by the fact that two-phase wetting phase relative permeabilities show little hysteresis between drainage and imbibition. Note also that Condition 3 is not strictly necessary, because both Eqs. 19 and 20 reduce to Condition 3 when $S_g \rightarrow S_g^I$.

Reduction in water permeability because of gas injection, as in Condition 1 above, is necessary for modeling pressure profiles from WAG experiments.

Points B, C, and D in Fig. 7 have not necessarily obtained irreducible water saturation before a new increasing water saturation process starts. For this case S_g^I must be calculated from

$$S_g^I = \left[\frac{k_{rw}^{W_1} - (k_{rw}^{\text{drain}})}{k_{rw}^{W_1} - k_{rw}^{W_2}}\right]_{(S_w)^{\text{end}}} (S_g)_{\max}. \quad \ldots\ldots\ldots\ldots\ldots\ldots (22)$$

With S_g^I estimated from Eq. 22, the secondary and subsequent water relative permeability curves for increasing water saturation can be found from Eq. 16. If S_{wi} is reached during a decreasing water saturation process, then S_w^I is known directly and must not be calculated from Eq. 22.

Additional saturation oscillations and new constrained trajectories can be handled by the equations above. But what if the first process starts with increasing water saturation? One plausible solution is to follow the increasing water saturation curve corresponding to the initial gas saturation.

4. $S_g = (S_g)_{\max}$ during a decreasing water saturation process. In this case, maximum reduction of water permeability is achieved, and water permeability is determined from the input given by a three-phase curve. It is only possible to leave this curve if gas is dissolved in the oil phase. Because the maximum gas saturation has occurred in the system, the corresponding minimum gas saturation will be $(S_{gr})_{\max}$. An indicator for condensation of gas can be that the gas saturation decreases below $(S_{gr})_{\max}$. This criterion is the only possible way a gridblock can leave the $k_{rw}^{W_2}$ curve. For this case,

$$(k_{rw}^{\text{drain}}) = k_{rw}^{W_2} \quad \ldots\ldots\ldots\ldots\ldots\ldots\ldots\ldots\ldots\ldots\ldots\ldots (23a)$$

$$\text{if} \quad (S_g - (S_{gr})_{\max}) > 0, \quad \ldots\ldots\ldots\ldots\ldots\ldots\ldots\ldots (23b)$$

and the next imbibition curve is given as

$$(k_{rw}^{\text{imb}}) = k_{rw}^{W_2}. \quad \ldots\ldots\ldots\ldots\ldots\ldots\ldots\ldots\ldots\ldots\ldots\ldots (24)$$

If gas is dissolved in the oil component, the water relative permeability curve must then be calculated from

$$(k_{rw}^{\text{drain}}) = k_{rw}^{W_1}\left(\frac{(S_{gr})_{\max} - S_g}{(S_{gr})_{\max}}\right) + k_{rw}^{W_2}\left(1 - \frac{(S_{gr})_{\max} - S_g}{(S_{gr})_{\max}}\right) \ldots\ldots (25a)$$

$$\text{if} \quad (S_g - (S_{gr})_{\max}) < 0 \ldots\ldots\ldots\ldots\ldots\ldots\ldots\ldots\ldots (25b)$$

Note that only the process for decreasing water saturation makes use of the gas saturation as a free variable, and the check for soluble gas is restricted to this process. The increasing water saturation process is constrained by the curves given in Fig. 6.

Intermediate Wetting Phase Hysteresis. The change in residual oil saturation with trapped gas observed in several experimental studies is included in the oil relative permeability description. We have used a Stone's Model 1 to calculate three-phase oil relative permeabilities. However, in our treatment of relative permeability, isoperms do not exist. The oil relative permeability is calculated in the numerical method by finding the corresponding trapped gas saturation from which the residual oil saturation is derived. The numerical routine must keep track of the saturation direction history in order to define the residual oil at a given oil saturation. The use of Stone's Model 1 in the calculation implies that the oil relative permeability will increase when the trapped gas saturation is increased and the residual oil is correspondingly reduced. The increased oil mobility is needed to model the fast oil mobilization in coreflood WAG displacements.[10, 24]

The consistent way of modeling residual oil in a numerical simulation is to replace S_{orw} in Eq. 8 with $(S_{or})_{S_{gt}=0}$, which is a three-phase zero isoperm. Here, the three-phase zero isoperm is a function of two saturations, generally, but can also be defined as a constant value (e.g., S_{orw}).

The residual oil can now be defined by the trapped gas according to

$$S_{or} = (S_{or})_{S_{gt}=0} - aS_{gt} \quad \ldots\ldots\ldots\ldots\ldots\ldots\ldots\ldots\ldots\ldots (26)$$

where a = a constant.

Three-phase oil relative permeability is, in this model, a function of both oil saturation and the saturation history, making it possible to account for process-dependent, intermediate-wetting relative permeability behavior.

Case Study. A two-dimensional simulation model is used to study the effect of cycle-dependent hysteresis. The simulation model represents a cross section of a reservoir with two vertical wells separated by 1000 m. The vertical height of the cross section is 100 m, and the vertical permeability is one-tenth of the horizontal permeability. The three-phase hysteresis settings are given in **Table 2**. A simulation model without hysteresis in relative permeability is used as a reference for the new model. The results from a simulation model with the Carlson[11] hysteresis are given in **Tables 3 and 4**. The effect of modifying residual oil saturation is studied in the case of the new cycle-dependent hysteresis models. The residual oil modification is observed to have minor effects on oil recovery for this case study.

The Carlson hysteresis model gives results nearly equal to those of the simulation model without any relative permeability hysteresis. However, a difference is seen in water breakthrough resulting from the reduced gas mobility. The trapping of gas in the Carlson model reduces the mobility to gas, which implies that the water production starts earlier. There is no hysteresis selected for the water phase. The same effect is observed from the cycle-dependent model, but the effect is even larger because the gas mobility is reduced by both trapping and gas saturation oscillation during three-phase flow. In addition, water mobility is reduced in the three-phase zone. Still, the water breakthrough is earlier for the cycle-dependent simulation. Such behavior can be explained by only a small area, which obtains cycle-reduced water permeability, and the decrease in gas production rate.

TABLE 2—CYCLE DEPENDENT HYSTERESIS

Land Constant	Gas Reduction Factor	k_{rw1}/k_{rw3}	Residual Oil Factor
3.4	4.9	1/10	1

TABLE 3—PRODUCTION RESULTS FROM A CROSS-SECTION MODEL

Simulation Model	Oil Production for 1,500/3,000 days (Sm^3)	Gas Production for 1,500/3,000 days (Sm^3)	Water Production for 1,500/3,000 days (Sm^3)
Base	57 000/85 000	32 500/80 000	0/12 500
Carlson	58 000/85 000	31 000/77 000	100/17 500
Cycle dependent	66 000/95 000	24 000/64 000	100/24 000
Cycle dependent without S_{or} model	65 000/92 000	23 000/61 000	150/23 500

TABLE 4—BREAKTHROUGH FROM A CROSS SECTION MODEL

Simulation Model	Gas Breakthrough (days)	Water Breakthrough (days)
Base	310	1850
Carlson	310	1580
Cycle dependent	310	1470
Cycle dependent without S_{or} model	310	1430

The cycle-dependent relative permeability model gives larger oil recovery than the other models, and the water breakthrough is at 1,470 days compared with 1,580 days for the Carlson model and 1,850 days for the base model.

Conclusions

1. Experimental data regarding three-phase flow have shown large variation in residual oil and endpoint relative permeabilities, depending on saturation history. A new form of saturation dependency for three-phase relative permeability is proposed.

2. Hysteresis models for three-phase relative permeability, which can account for irreversible scanning curves during three-phase flow, are developed. The nonwetting phase relative permeability is history dependent on both the nonwetting phase saturation and the wetting phase saturation. The wetting phase relative permeability is history dependent on the nonwetting phase saturation. Both wetting and nonwetting phase relative permeabilities are functionally dependent on the respective phase saturation. The three-phase models are consistent with trends in experimental data.

3. An expression for residual oil accounting for trapped gas in a Stone Model 1 formulation is suggested. In this case, the oil relative permeability becomes process dependent, and large hysteresis for low oil saturation can occur. In processes where trapping of gas is significant, very low residual oil saturations can be achieved. Hysteresis in oil relative permeability decreases with increasing oil saturation.

4. A new general form of saturation dependency for three-phase relative permeability is proposed, based on recently published research regarding three-phase pore-level displacements. The new representation uses the initial saturation at the start of a given process. Hysteresis is assumed to occur between constrained trajectories.

5. It is argued that changes in gas relative permeability in experiments involving different spreading conditions can be compatible with hysteresis in three-phase gas relative permeability and residual oil behavior because of process dependence. It is suggested that the same pore phenomenon dominates the fluid flow behavior for these two types of experiments, and the same qualitative trends in gas relative permeability and residual oil are found from the experimental data.

6. The new cycle-dependent relative permeability models give larger oil recovery than does simulation without relative permeability hysteresis or with a two-phase gas hysteresis model in the presented simulation example. The increase in oil recovery is mainly caused by the reduced gas mobility in the studied cross-section model.

Nomenclature

a = constant
C = Land constant
G_1 = primary gas injection
G_2 = secondary gas injection
G_3 = tertiary gas injection
k_{rg}^{drain} = unknown drainage scanning curve as a function of S_g
k_{rg}^{input} = primary gas relative permeability curve, G_1, given as input
k_{rg}^{imb} = scanning curve for decreasing gas saturation (imbibition)
k_{ri} = relative permeability for Phase i
n = number of hysteresis loops performed at the system studied (a hysteresis loop always starts with an increasing gas saturation process)
S = saturation
S_w^{I} = water saturation when the system is shifting from a decreasing gas saturation process to an increasing gas saturation process
S_g^{start} = gas saturation when the system is shifting from a decreasing gas saturation process to an increasing gas saturation process
S_{wi} = irreducible water saturation
W_1 = primary water injection
W_2 = secondary water injection
W_3 = tertiary water injection
α = reduction exponent given as input
ε = tolerance limit
σ = interfacial tension

Subscripts

g = gas
gi = initial gas saturation for trapped gas calculations
gf = free gas saturation
gr = trapped gas saturation
n = number of hysteresis loops
or = residual oil
orw = residual oil to water
w = water
wi = irreducible water saturation

Superscripts

α = reduction exponent
I = initial
drain = drainage
end = end of hysteresis loop
imb = imbibition
input = input to numerical routine
start = start of hysteresis loop
trans = transformed

Acknowledgments

The authors thank Norsk Hydro for permission to publish this work and G. Bowen of Geoquest for useful comments.

References

1. Stone, H.L.: "Estimation of Three-Phase Relative Permeability," *J. Cdn. Pet. Tech.* (February 1970) 214.
2. Yadav, G.D. *et al.*: "Microscopic Distribution of Wetting and Nonwetting Phases in Sandstones During Immiscible Displacements," *SPERE* (May 1987) 137.
3. Øren, P.E. and Pinczewski, W.V.: "The Effect of Film-Flow on the Mobilization of Waterflood Residual Oil by Gas Flooding," 1991 IOR Symposium, Stavanger, 21–23 May.
4. Øren, P.E. and Pinczewski, W.V.: "Fluid Distribution and Pore-Scale Displacements in Drainage Dominated Three-Phase Flow," *Transport in Porous Media* (1995) **20,** 105.
5. Vizika, O. and Lombard, J-M.: "Wettability and Spreading: Two Key Parameters in Oil Recovery With Three-Phase Gravity Drainage," paper SPE 28613 presented at the 1994 SPE Annual Technical Conference and Exhibition, New Orleans, 25–28 September.
6. Blunt, M.J., Fenwick, D.H., and Zhou, D.: "What Determines Residual Oil Saturation in Three-Phase Flow?" paper SPE 27816 presented at the 1994 Improved Oil Recovery Symposium, Tulsa, Oklahoma, 17–20 April.
7. Fenwick, D.H. and Blunt, M.J.: "Three Dimensional Modelling of Three Phase Imbibition and Drainage," *Advances in Water Resources* (1997) **21,** No. 2, 121.
8. Fenwick, D.H. and Blunt, M.J., 1995: "Pore Level Modelling of Three Phase Flow in Porous Media," presented at the 1995 8th European IOR Symposium in Vienna, Austria, 15–17 May.
9. Skauge, A. and Aarra M.: "Effect of Wettability on the Oil Recovery by WAG," presented at the 1993 7th IOR Symposium in Moscow, 26–28 October.
10. Skauge, A. and Larsen, J.A.: "Three-Phase Relative Permeabilities and Trapped Gas Measurements Related to WAG Processes," paper 9421 presented at the 1994 Intl. Symposium of the Soc. of Core Analysts, Stavanger, 12–14 September.
11. Carlson, F.M.: "Simulation of Relative Permeability Hysteresis to the Nonwetting Phase," paper SPE 10157 presented at the 1981 SPE Annual Technical Conference and Exhibition, San Antonio, Texas, 4–7 October.
12. Killough, J.E.: "Reservoir Simulation with History-Dependent Saturation Functions," *SPEJ* (February 1976); *Trans.*, AIME, **261.**
13. Stone, H.L.: "Estimation of Three-Phase Relative Permeability and Residual Oil Data," *J. Cdn. Pet. Tech.* (October–December 1973), 53.
14. Oak, M.J.: "Three-Phase Relative Permeability of Berea Sandstone," paper SPE 20183, presented at the 1990 SPE/DOE Symposium on Enhanced Oil Recovery, Tulsa, Oklahoma, 22–25 April.
15. Salter, S.J. and Mohanty, K.K.: "Multiphase Flow in Porous Media: I. Macroscopic Observations and Modeling," paper SPE 11017 presented at the 1982 SPE Annual Technical Conference and Exhibition, New Orleans, 26–29 September.
16. Jerauld, G.R. and Salter, S.J.: "The Effect of Pore-Structure on Hysteresis in Relative Permeability and Capillary Pressure: Pore-Level Modeling," *Transport in Porous Media*, Vol. 5, (1990).
17. Naar, J., Wygal, R.J., and Henderson, J.H.: "Imbibition Relative Permeability in Unconsolidated Porous Media," *SPEJ* (March 1962) 13.
18. Batycky, J.P. and McCaffrey, F.G.: "Low Interfacial Tension Displacement Studies," paper 78-29-26 presented at the 1978 29th Annual Meeting of Petroleum Soc. of CIM, Calgary, 13–16 June.
19. Fenwick, D.H.: "Pore Scale Modeling of Three-Phase Flow," PhD dissertation, Stanford U., California, February 1997.
20. Munkerud, P.K., Duquerroix, J.P., and Virnovski, G.: "Gas Mobility During Three-Phase Flow in Combined Gas/Water Injection Processes," *RUTH, a Norwegian Research Program on Improved Oil Recovery, Program Summary*, S.M. Skaeveland, A. Skauge, L. Hinderaker, and C.D. Sisk (eds.), Norwegian Petroleum Directorate, Stavanger (1996).
21. Geffen, T.M. *et al.*: "Experimental Investigation of Factors Affecting Laboratory Relative Permeability Measurements," *Trans.*, AIME (1951) **191.**
22. Osoba, J.S. *et al.*: "Laboratory Measurements of Relative Permeability," *Trans.*, AIME (1951) **191.**
23. Kyte, J.R. *et al.*: "Mechanism of Waterflooding in the Presence of Free Gas," *Trans.*, AIME (1956) **207.**
24. Holmgren, C.R. and Morse, R.A.: "Effect of Free Gas Saturation on Oil Recovery by Waterflooding," *Trans.*, AIME (1951) **192.**
25. Dyes, A.B.: "Production of Water-Driven Reservoirs Below Their Bubble Point," *Trans.*, AIME (1954) **201.**
26. Dardaganian, S.G.: "The Displacement of Gas by Oil in the Presence of Connate Water," MS thesis, Texas A&M U., College Station, Texas (1957).
27. Crowell, D.C., Dean, G.W., and Loomis, A.G.: "Efficiency of Gas Displacement From a Water-Drive Reservoir," RI 6735, USBM (1966).
28. Land, C.S.: "Calculation of Imbibition Relative Permeability for Two- and Three-Phase Flow," *SPEJ* (June 1968); *Trans.*, AIME (1968) **243.**
29. Evrenos, A.I. and Comer, A.G.: "Sensitivity Studies of Gas-Water Relative Permeability and Capillarity in Reservoir Modeling," paper SPE 2668 presented at the 1969 SPE Annual Fall Meeting, Denver, Colorado, 28 September–1 October.
30. Colonna, J., Brissard, F., and Millet, J.L.: "Evolution of Capillary and Relative Permeability Hysteresis," *SPEJ* (February 1972) 28; *Trans.*, AIME, **253.**
31. Eikje, E. *et al.*: "Relative Permeability Hysteresis in Micellar Flooding," presented at the 1991 6th European IOR Symposium, Stavanger, 21–23 May.
32. Virnovskii, G.A.: "Determination of Relative Permeabilities in a Three-Phase Flow in a Porous Medium," Translated from *Izvestiya Akademii Nauk SSSR, Mekhanika Zhidkosti i Gaza*, Moscow (September–October 1984) No. 5, 187.
33. Kvanvik, B.A. *et al.*: "Three-Phase Microemulsion Relative Permeabilities Experimental and Theoretical Considerations," presented at the 1991 6th European IOR Symposium, Stavanger, 21–23 May.
34. Patel, P.D., Christman, P.G., and Gardner, J.W.: "An Investigation of Unexpectedly Low Field-Observed Fluid Mobilities During Some CO_2 Tertiary Floods," *SPERE* (November 1987) 507.
35. Schneider, F.N. and Owens, W.W.: "Relative Permeability Studies of Gas-Water Flow Following Solvent Injection in Carbonate Rocks," *SPEJ* (February 1976) 23.
36. Hawkins, J.T. and Bouchard, A.J.: "Reservoir-Engineering Implications of Capillary-Pressure and Relative-Permeability Hysteresis," *The Log Analysts* (July–August 1992), 415.
37. Braun, E.M. and Holland, R.F.: "Relative Permeability Hysteresis: Laboratory Measurements and a Conceptual Model," *SPERE* (August 1995) 222.
38. Wei, J.Z. and Lile, O.B.: "Influence of Wettability and Saturation Sequence on Relative Permeability Hysteresis in Unconsolidated Porous Media," paper SPE 25282 available from SPE Customer Service, Richardson, Texas (1993).
39. Amaefule, J.O. and Handy, L.L.: "The Effect of Interfacial Tensions on Relative Oil/Water Permeabilities of Consolidated Porous Media," *SPEJ* (June 1982) 371.
40. Torabzadeh, S.J. and Handy, L.L.: "The Effect of Temperature and Interfacial Tension on Water/Oil Relative Permeability of Consolidated Sand," paper SPE 12689 presented at the 1984 SPE/DOE Symposium on Enhanced Oil Recovery, Tulsa, Oklahoma 15–18 April.
41. Fulcher, R.A., Ertekin, T., and Stahl, C.D.: "The Effect of the Capillary Number and Its Constituents on Two-Phase Relative Permeability Curves," paper SPE 12170 presented at the 1983 SPE Annual Technical Conference and Exhibition, San Francisco, 5–8 October.
42. Wang, F.H.L.: "Effect of Wettability Alteration on Water/Oil Relative Permeability, Dispersion, and Flowable Saturation in Porous Media," *SPERE* (May 1988) 617.
43. Fayers, F.J.: "Evaluation of Normalized Stone's Methods for Estimating Three-Phase Relative Permeabilities," *SPEJ* (April 1984) 224.
44. Baker, L.E.: "Three-Phase Relative Permeability Correlations," paper SPE 17369 presented at the 1988 SPE/DOE Enhanced Oil Recovery Symposium, Tulsa, Oklahoma, 17–20 April.
45. Larsen, J.A. and Skauge, A.: "Comparing Hysteresis Models for Relative Permeability in WAG Studies," paper 9506 presented at the 1995 Intl. Symposium of the Soc. of Core Analysts, San Francisco, 12–14 September.
46. Skauge, A. and Larsen, J.A.: "A New Approach to Model the WAG Process," presented at the 1994 15th IEA Collaborative Project on Enhanced Oil Recovery, Bergen, Norway, 28–31 August.
47. Stone, H.L.: "Vertical Conformance in an Alternating Water-Miscible Gas Flood," paper SPE 11130 presented at the 1982 SPE Annual Technical Conference and Exhibition, New Orleans, 26–29 September.

48. Jenkins, M.K.: "An Analytical Model for Water/Gas Miscible Displacements" paper SPE 12632 presented at the 1984 SPE/DOE Symposium on Enhanced Oil Recovery, Tulsa, Oklahoma, 15–18 April.
49. Guzman, R.E. *et al.*: "Three-Phase Flow in Field-Scale Simulations of Gas and WAG Injections," paper SPE 28897 presented at the 1994 SPE European Petroleum Conference, London, 25–27 October.
50. Fayers, F.J.: "Extension of Stone's Method I and Conditions for Real Characteristics in Three-Phase Flow," *SPERE* (November 1989) 437.
51. Kortekaas, F.M. and Poelgeest, F.: "Liberation of Solution Gas During Pressure Depletion of Virgin and Watered-Out Oil Reservoirs," *SPERE* (August 1991) 329.

Appendix—Algorithm

Input.

primary drainage curve (gas)
Land constant; C
reduction coefficient; α
tolerance limits; ε

Startup.

S1. **if** decreasing nonwetting saturation **then** $n = 0$

—Calculate the corresponding amount of trapped gas upon a total decreasing gas saturation process,

$$S_{gr} = \frac{S_{gi}}{1 + CS_{gt}}.$$

—Estimate free nonwetting saturation,

$$S_{gf} = \frac{1}{2}\left[(S_g - S_{gr}) + \sqrt{(S_g - S_{gr})^2 + \frac{4}{C}(S_g - S_{gr})}\right].$$

—Find imbibition relative permeability from

$$[k_{rg}^{\text{imb}}(S_g) = k_{rg}^{\text{input}}(S_{gf})]_{k=1}$$

Goto hysteresis loop H2, $n = 1$

S2. **if** increasing nonwetting saturation **then** $n = 1$

—Calculate drainage curve from

$$k_{rg}^{\text{drain}}(S_g; S_w^{\text{start}}) = [k_{rg}^{\text{input}}(S_g)]*\left[\frac{S_{wi}}{S_w}\right]^{\alpha}$$

goto hysteresis loop H1

Hysteresis loop.

H1. **if** $S_{n,\ \text{timestep}=n} + \varepsilon < S_{n,\ \text{timestep}=n-1}$ **then** activate imbibition procedure

—Estimate S_{gr} associated to the inflection point,

$$\left[S_{gr} = \frac{1}{C + 1/S_{gi}}\right]_n.$$

—check for

$$(S_{gr})_n > (S_{gr})_{n-1} \Rightarrow S_{gr} = (S_{gr})_n$$

$$(S_{gr})_n < (S_{gr})_{n-1} \Rightarrow S_{gr} = (S_{gr})_{n-1}$$

—Estimate transformed values,

$$(S_{gr}^{\text{trans}})_n = (S_{gr})_n - (S_g^{\text{end}})_{n-1},$$

$$(S_{gi}^{\text{trans}})_n = (S_{gi})_n - (S_g^{\text{end}})_{n-1},$$

$$(C^{\text{trans}})_n = \frac{1}{(S_{nt}^{\text{trans}})_n} - \frac{1}{(S_{ni}^{\text{trans}})_n},$$

$$S_{gf} = \left[\frac{1}{2}(S_g - S_{gt}) + \sqrt{(S_g - S_{gt})^2 + \frac{4}{C^{\text{trans}}}(S_g - S_{gt})}\right]_n.$$

—Estimate effective free saturation,

$$(S_{gf}^{\text{trans}})_n = (S_{gf})_n + (S_n^{\text{end}})_{n-1}.$$

—Estimate imbibition relative permeability

$$[k_{rg}^{\text{imb}}(S_g) = k_{rg}^{\text{drain}}(S_{gf}^{\text{trans}})]_n.$$

—$n = n + 1$

H2. **if** $S_{n,\ \text{timestep}=n} + \varepsilon > S_{n,\ \text{timestep}=n-1}$ **then** activate drainage procedure

—**if** $\Delta S_g^{\text{imb}} \geq \Delta S_o^{\text{imb}} + \varepsilon$ and $S_w^{\text{end,imb}} < S_w^{\max}$ **then** no new hysteresis loop is generated

else estimate drainage relative permeability from

$$k_{rg}^{\text{drain}}(S_g; S_w^{\text{start}}) = [k_{rg}^{\text{input}}(S_g) - k_{rg}^{\text{input}}(S_g^{\text{start}})]_n*\left[\frac{S_{wi}}{S_w^{\text{start}}}\right]^{\alpha} + [k_{rg}^{\text{imb}}(S_g^{\text{start}})]_{n-1}.$$

H3. goto H1

Johne A. Larsen works at Norsk Hydro A/S. Address: Norsk Hydro A/S, Sandsliveien 90, N-5020 Bergen, Norway, e-mail: Alex.Larsen@nho.hydro.com. Photograph is unavailable. **Arne Skauge** is a department manager with Norsk Hydro A/S. Address: Norsk Hydro A/S, Sandsliveien 90, N-5020 Bergen, Norway, e-mail: arne.skauge@nho.hydro.com. He is a member of the Editorial Review Committee and was a 1993–94 member of the Improved Oil Recovery Symposium Program Committee.

Skauge